An Investigation of Structural-Mechanical Properties of Spun-Bonded Non-Woven Using Computer Vision Method

Mina Emadi, Mohammad Ali Tavanaie*, and Pedram Payvandy

Abstract- This paper aims at the measurement of surface uniformity, thermally-bonded points, distribution of fibers orientation and local displacement in tensile testing for spun-bonded nonwoven polypropylene fabrics. For this purpose, an image processing method was used to produce clustered images based on the k-means clustering algorithm along with Davies-Bouldin index and the PSNR image quality evaluation method. Then, the quadrant method for surface uniformity, an image processing method based on morphological operators for uniformity of thermally-bonded points, the regionprops function (RF) method for distribution of fiber orientation and the digital image correlation (DIC) method for local displacement were used to calculate the parameters of nonwoven samples. Also, the relationships between image processing and the experimental results of tensile tests were studied. The results indicated that the structural properties of a fabric, such as surface uniformity, bonded structure, distribution of fiber orientation and critical points, have great impacts on its tensile properties at the selected weights and non-uniformity levels. Hence, a sample with a higher level of uniformity and, consequently, more regular bonding points with a higher bonding percentage, better distribution of fiber orientation and less critical points offers the best tensile properties.

Keywords: image processing, k-means clustering, regionprops function, digital image correlation, tensile properties, spun-bonded non-woven fabric

I. INTRODUCTION

In recent years, the application of computer vision technology in the textile industry has increased significantly. Nowadays, indeed, the technique is applied for various purposes, such as size assessment, calibration, transportation, production quality enhancement, inspection, grading, sorting, and separation. Determination of fabric properties and online controls, such as control of web uniformity [1], defects [2], fiber diameter [3], and fiber orientation [4] are among the tasks that image processing systems can take over. This wide range of applications is due to the fact that computer vision systems provide significant amounts of information about the nature or attributes of scene analyses. Furthermore, this technology makes it possible to study scenes in regions where the human eye is not sensitive enough. Determining the properties of non-woven plays a substantial role in the extensive use of these fabrics for new applications. Since the term 'uniformity' is defined as an index of variation in such aspects as fiber orientation, weight, thickness, density, and fiber diameter, the constancy or inconstancy of the measured values of these features in different locations of a non-woven web can be referred to as 'uniformity' or 'non-uniformity'.

There is a lot of research on the non-woven uniformity based on online measurements. Some researchers have used optical methods to evaluate changes in the basic weight. Veerabadran *et al.* examined a technique in which images and their optical densities were used to provide a uniformity index [5]. A similar trend was pursued by Boeckerman. In his study, the non-woven fabrics were subjected to a transmitted light, a camera recorded the image intensity, and the sample optical density was related to the web weight [6]. In such techniques, the uniformity index is calculated by using the coefficient of variation (CV%) of the optical density, and measurements on various scales offer different indicators. Lien *et al.* used optical intensity for online basic weight assessment, which, like other studies, it had an inherent problem in that it relied on size [7]. To determine the level of non-uniformity, wavelet analysis and LVQ neural network [8], Bayesian [9], and the generalized Gaussian density model [10] were used. One of the studies to defeat the size reliance impediments in the coefficient of variation (CV%) analysis has been done by Pourdeyhimi *et al.* who defined a uniformity index by combined image processing and the quadrant method [11]. Amir Nasr *et al.* conducted a study to measure the uniformity of non-wovens with the known quadrant method

M. Emadi, M.A. Tavanaie, and P. Payvandy
Department of Textile Engineering, Faculty of Engineering, Yazd University, Yazd, Iran.

Correspondence should be addressed to M.A. Tavanaie
e-mail: ma.tavanaie@yazd.ac.ir

[12]. In studies by Nohut *et al.* [13] and Taskan *et al.*[14], digital image analysis and artificial neural network were used to predict the weight, tensile strength and elongation at the break values of the polypropylene non-woven fabrics with various weights.

Many studies confirm that fiber orientation extremely influences the properties of textile products. For example, Maoa *et al.* [15] pointed that fiber orientation is a main factor influencing non-woven anisotropy. Murugan and Ramakrishna [16] showed that the orientation of fibers is one of the most important features of a perfect tissue scaffold made of nanofibers. Accordingly, measurement of fiber orientation is an important part of quantitative measurements in the field of textiles. In this context, one can refer to a specially influencing series of papers by Pourdeyhimi *et al.* [17-22] dedicated to measuring fiber orientations. Also, Tunák *et al.* [23] focused on estimating the fiber orientation of nano-fibrous and nonwoven layers. They studied four methods, including rose of directions, spectral approach, moment approach, and a combination of spectral and moment approaches for estimation of fibers orientation. The results indicated that the proposed method can be effectively used to estimate the directional orientation of fibrous textile materials in terms of their homogeneity, eventual defects, random violation of regularity of the structure, etc. Stolyarov *et al.* [24] studied an analysis system to evaluate fiber orientations in nonwoven structures and to establish the relationship between the structure and the mechanical behavior of nonwoven fabrics. In their study, an interpretation was provided of the fiber deformation mechanism in the internal structure of nonwoven fabrics, and a coefficient of anisotropy was proposed for the internal structure of nonwoven materials under tension.

Measuring the surface deformation of structures subjected to mechanical loadings is an important task of mechanics. One of the most commonly used powerful and flexible tools for surface deformation measurement is digital image correlation (DIC). It directly provides full-field displacements and strains by comparing the digital images of the specimen surface in non-deformed (or reference) and deformed states, respectively. During recent years, the DIC method has been widely studied and improved to achieve high accuracy in deformation measurements. Peters *et al.* [25] studied the digital image correlation (DIC) technique commonly used in experiments as an effective tool for full-field deformation measurements. Furthermore, Zhou *et al.* [26] suggested that the DIC method is easy to use and can provide suitable resolution of displacement and strain fields. According to Koerber *et al.* [27], the DIC technique can be used for quasi-static and high strain rate experiments in order to obtain the in-plane strain field over the entire surface of a specimen. Finally, Pierron *et al.* [28] used a high-speed camera in a high-strain-rate test, in which sample deformation was tested and the field method of a 3-point bending was evaluated.

In this study, we have evaluated the overall surface uniformity of different samples using the quadrant method. The k-means clustering method is applied to produce binary images. Also, proposed image processing methods are used to calculate the uniformity of thermally-bonded points. The fiber orientation distribution is measured by regionprops function and the local displacement during tensile testing is evaluated by digital image correlation method. It is attempted to achieve an interaction between the tensile properties of non-woven fabrics and the non-woven dispersion indexes. To reach this end, the tensile properties of the non-woven samples are measured, and then the experimental data are compared with the data obtained from the image processing method. In textile factories, strength measurement is usually done offline. Choosing this technique is effective because image processing systems can be applied to determine a uniformity index quickly and to do calculations fast and efficiently. This makes it significant to develop a technique for online applications. Applying the image processing method in online quality control is a very useful and effective method that can help the owners of factories to save time and money. Noticing a variation in the quality of a product, one can find out the lack of uniformity. It leads to quick corrections in the production line and, thus, prevention of large amounts of shoddy products.

II. EXPERIMENTAL

A. Materials

Two sets of thermally bonded non-woven fabric were taken directly from a roll of a factory polypropylene fabric. Samples were prepared by changing degree of fiber dispersion, which led to different uniformity levels (poor–medium–good) and two different weights ($15 \, g/m^2$, $30 \, g/m^2$). The bonding temperature was 165 °C, the nip pressure was varied from $3 \, kg/cm^2$ to $3.2 \, kg/cm^2$ for two types of the samples, and production speed of the samples was 40 m/min. The samples were cut from different stances of the web and then weighted. The average weight and thickness (ASTM D5729) of 10 specimens and the CV% for each fabric type are presented in Table I.

B. Methods

B.1. Tensile Test

For analysis of the mechanical properties of non-woven fabrics, 10 specimens were selected from each sample

TABLE I
AVERAGE WEIGHT, THICKNESS AND CV% OF THERMALLY-BONDED NON-WOVEN POLYPROPYLENE

	S15-1	S15-2	S15-3	S30-1	S30-2	S30-3
Uniformity degree	Good	Medium	Poor	Good	Medium	Poor
Average weight (g/m^2)	15.653	15.690	15.801	30.427	32.861	31.934
(CV%)	(3.15)	(5.27)	(5.37)	(3.88)	(5.56)	(9.22)
Average thickness (mm)	0.161	0.206	0.207	0.270	0.314	0.317
(CV%)	(7.24)	(8.39)	(9.15)	(2.94)	(11.3)	(22.88)

(Table I). The stress and strain at peak were tested according to the standard ASTM D5034 using a tensile strength tester (INSTRON). The measuring conditions were as follows: the speed of the clamps 150 mm/s, distance between the clamps of the tensile strength tester 150 mm and temperature 20±2 °C, Rh 50±5%.

B.2. Image Processing
A scanner with a resolution of 2400 dpi was used to obtain images of the structure of non-woven fabrics. The advantage of using the scanner in obtaining fabric images is that it has a high depth of field even at high magnifications. Using scanner, more fibers in the fabric are focused and included in the image compared with other methods. For this imaging method, a black screen was placed behind the samples and all the image dimensions were limited to 10×15 cm^2. Three levels of the non-woven samples uniformity are shown in Fig. 1.

B.3. Surface Uniformity Measurement
For surface uniformity measurement, the color images of the samples were converted into grayscales and, afterward, a thresholding operation was done. The k-means clustering method was applied to convert color images to grey scales, and then black-and-white ones [29]. In addition, the Davies-Bouldin index was used for cluster validation [30]. The non-woven sample images were divided into 3-6 intensities or clusters. The k-means clustering method was performed 10 times for each image, and, then, the best one among 10 clusterings was selected using Davies-Bouldin index. After converting the best of clustered images to a binary image and making four binary images, the PSNR index was applied to choose the best binary image [31]. After thresholding, the quadrant method was applied on each input image to assess the surface dispersion index of the non-woven samples. In the quadrant method, the image was divided into squares and analyzed. The average number of white pixels in a square, the total average of white pixels as the average value of the fiber fraction in surface, the standard deviation of them, and their dispersion index were calculated. The surface dispersion index was calculated by the average number of white pixels and used as a criterion to determine the surface uniformity of the non-woven fabrics.

B.4. Thermally-Bonded Points Uniformity Measurement
For measuring the uniformity of thermally-bonded point, the color images were converted into grayscales. The bit plane slicing was applied to those grayscales to take out the best bit plane, which contains more visual information of the thermally-bonded points. The highest-order planes contain a great deal of valuable visual data, while the lower-order planes include finer details of the image. So, a bit plane which provides more visual information of the thermally-bonded points was selected. This plane was used as a selected binary image for further analysis. In
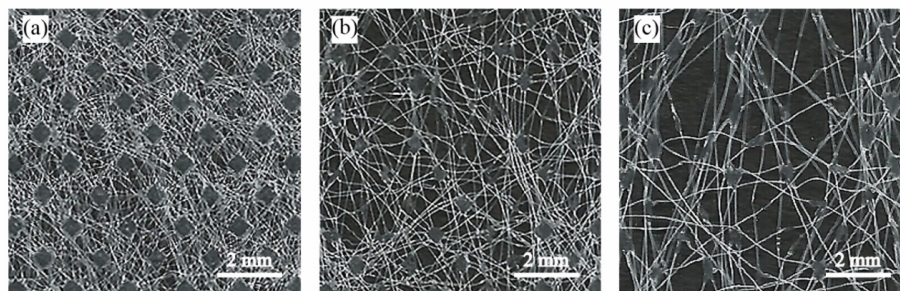

Fig. 1. Three levels of 15 g/m^2 samples uniformity: (a) sample with the highest uniformity, (b) sample with the medium uniformity, and (c) sample with the lowest uniformity.
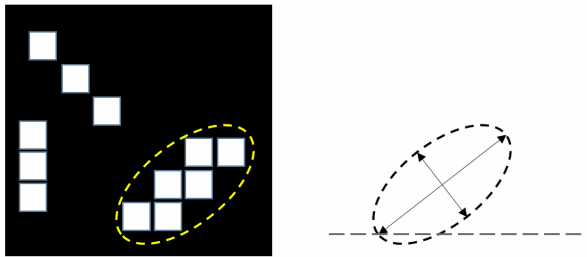
Fig. 2. Fiber orientation measurement by regionprops function (RF).

the next step, the negative binary image of the bit plane was created and exposed to opening and closing functions as well as median filtering so as to remove undesirable details. Finally, the thermally-bonded points were visible as white objects on a black background in the final binary image. The area of each bonding point, the percentage of the bonded area and the average area of bonding points were calculated. Then, the dispersion index of the bonding points area (I_d) which presents the amount of dispersion of the bonding points area was calculated to evaluate the uniformity of the bonding points.

B.5. Fiber Orientation Measurement
After thresholding and conversion of the non-woven images to black and white through k-means clustering, the images were used to measure the distribution of fiber orientation. A MATLAB image processing toolbox was provided for the regionprops image analysis. Generally, the regionprops function (RF) method is used to extract the feature of ellipse regions in an image of function, especially to characterize the orientation of the ellipse regions. In this technique, a scalar is specified to the angle between the x-axis and the major axis of the ellipse to measure fiber orientation. The value is in degrees, ranging from -90 degrees to 90 degrees. Fig. 2 illustrates the axes and orientation of an ellipse. The left side of the figure shows an image region and its corresponding ellipse. On the right side, the same ellipse is shown with solid lines representing the axes, the dots are the foci, and the orientation is the angle between the horizontal dotted line and the major axis.

B.6. Local Displacement Measurement During Tensile Testing
The displacement of different locations in the non-woven sample during tensile testing was calculated by the digital image correlation (DIC) method [32] based on the local displacements detected in a series of consecutive images obtained in different states, one before deformation and the others after deformation. Surface patterns on the test specimen are essential for this technique. In order to create a
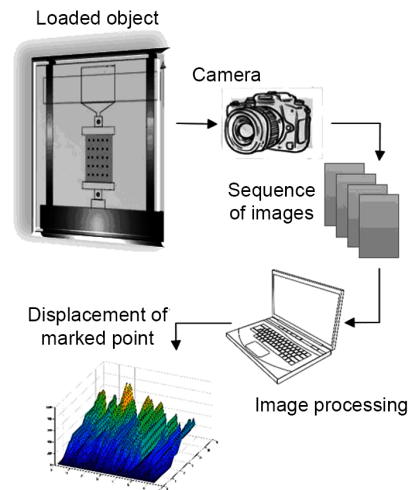

Fig. 3. Local displacement measurement during tensile testing.

characteristic pattern on the specimen surface, black dots were deposited regularly on the surface background. The specimens were fixed to a mechanical testing machine in conditions similar to those of tensile testing. Tensile testing was done, and a sequence of images was taken by a high speed camera. The images were given to the MATLAB software to implement the DIC method, and the local displacement of the marked points was calculated (Fig. 3).

III. RESULTS AND DISCUSSION

A. Thresholding Results
Typical thresholding is one of the most common methods that can be applied when the pixel intensity distribution of objects differs from that of the background. The background in the non-woven sample images with different intensities is not clear and distinct. Thus, the process of turning them into binary images through typical thresholding can destroy a lot of details. One thing that can overcome this limitation is the k-means clustering method. After converting the best of 3-6 clustered images to binary ones and making four binary images, 4 clusters were selected as the best number of clusters with the highest PSNR indices. The thresholding images for S15-3 sample are shown in Fig. 4. The PSNR and Davies-Bouldin index values for 4 clusters are presented in Table II. The binary image obtained from the clustering method was selected for future analysis.

B. Surface Uniformity Results
The non-woven samples were cut into the sizes shown in Table III and then were weighed. The weight dispersion index values were calculated to verify the data obtained from the image processing method (quadrant method). Two dispersion index values were obtained
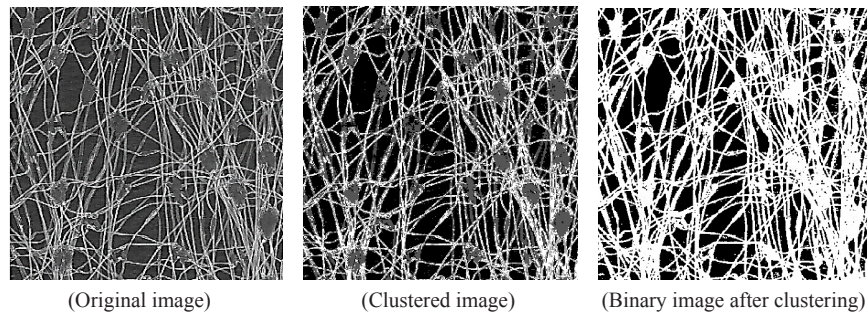
(Original image)   (Clustered image)   (Binary image after clustering)

Fig. 4. Thresholding operations for S15-3 sample.

TABLE II
PSNR AND DAVIES-BOULDIN INDEX VALUES FOR 4 CLUSTERS

	S15-1	S15-2	S15-3	S30-1	S30-2	S30-3
PSNR	6.6296	6.9211	7.2438	8.3098	8.1069	9.1187
DB	0.4153	0.4330	0.4422	0.4469	0.4522	0.4352

from the image processing method and weighing. The corresponding correlation coefficients are presented in Table III. As it can be seen, the correlation coefficient values for all the samples are higher than 0.95. Generally, a correlation coefficient shows the relationship between two variables. So, coefficient values greater than 0.95 show a strong and positive relationship between the image processing and the weighing methods. The results of the image processing method were well correlated with the weighing results. They were also compatible with the degree of sample visual uniformity. Therefore, it is realized that, in each group with the same weighted

TABLE III
SURFACE DISPERSION INDEX OF QUADRANT METHOD AND WEIGHING AND THEIR CORRELATION COEFFICIENTS

	Size of squares (cm²)	S15-1	S15-2	S15-3	S30-1	S30-2	S30-3
Image processing surface dispersion index	5×5	0.0134×10^{-2}	0.3467×10^{-2}	0.2075×10^{-2}	0.0053×10^{-2}	0.0378×10^{-2}	0.1757×10^{-2}
	2.5×2.5	0.1646×10^{-2}	0.4406×10^{-2}	0.3313×10^{-2}	0.0128×10^{-2}	0.0532×10^{-2}	0.2982×10^{-2}
	1.25×1.25	0.3041×10^{-2}	0.5682×10^{-2}	0.7182×10^{-2}	0.0215×10^{-2}	0.0712×10^{-2}	0.4159×10^{-2}
Weighting dispersion index	5×5	0.0188	0.0614	0.1333	0.1291	0.7867	1.0112
	2.5×2.5	0.0592	0.1055	0.1922	0.2036	1.0190	1.6223
	1.25×1.25	0.1388	0.2882	0.3242	0.5788	1.6172	2.3254
Correlation coefficient		0.9704	0.9639	0.9957	0.9972	0.9595	0.9973

(Original image)   (The 6th bit-plane)   (Final image)
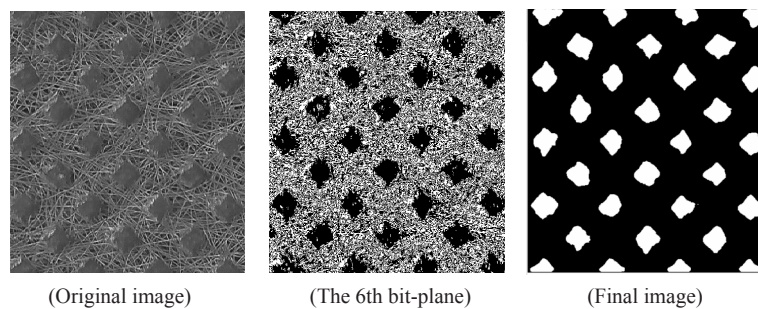
Fig. 5. Bonding points extraction.

TABLE IV
PARAMETERS OF THERMALLY-BONDED POINTS OBTAINED FROM THE IMAGE PROCESSING METHOD

	S15-1	S15-2	S15-3	S30-1	S30-2	S30-3
Bonding average area (mm²)	0.3023	0.2424	0.2190	0.3642	0.3403	0.1475
Bonding dispersion index	1.2456	3.0454	7.7126	1.2626	2.1874	4.7308
Bonding percentage (%)	13.0093	10.9609	8.8300	18.4674	15.9942	7.0715

average, the lower degree of sample surface uniformity causes the higher dispersion index. It seems that the quadrant method is an appropriate method to determine the surface uniformity of the non-woven fabrics. The similar results were presented in the Nohut *et al.* [13] and Taskan *et al.* [14] studies.

C. Thermally-Bonded Points Uniformity Results

As Fig. 5 shows, the 6th bit plane, compared to the other bit planes, reveals the best information about the thermally-bonded points. So, it could be used as a selected binary image for subsequent analyses. The final image is a binary image in which the thermally-bonded points are visible as
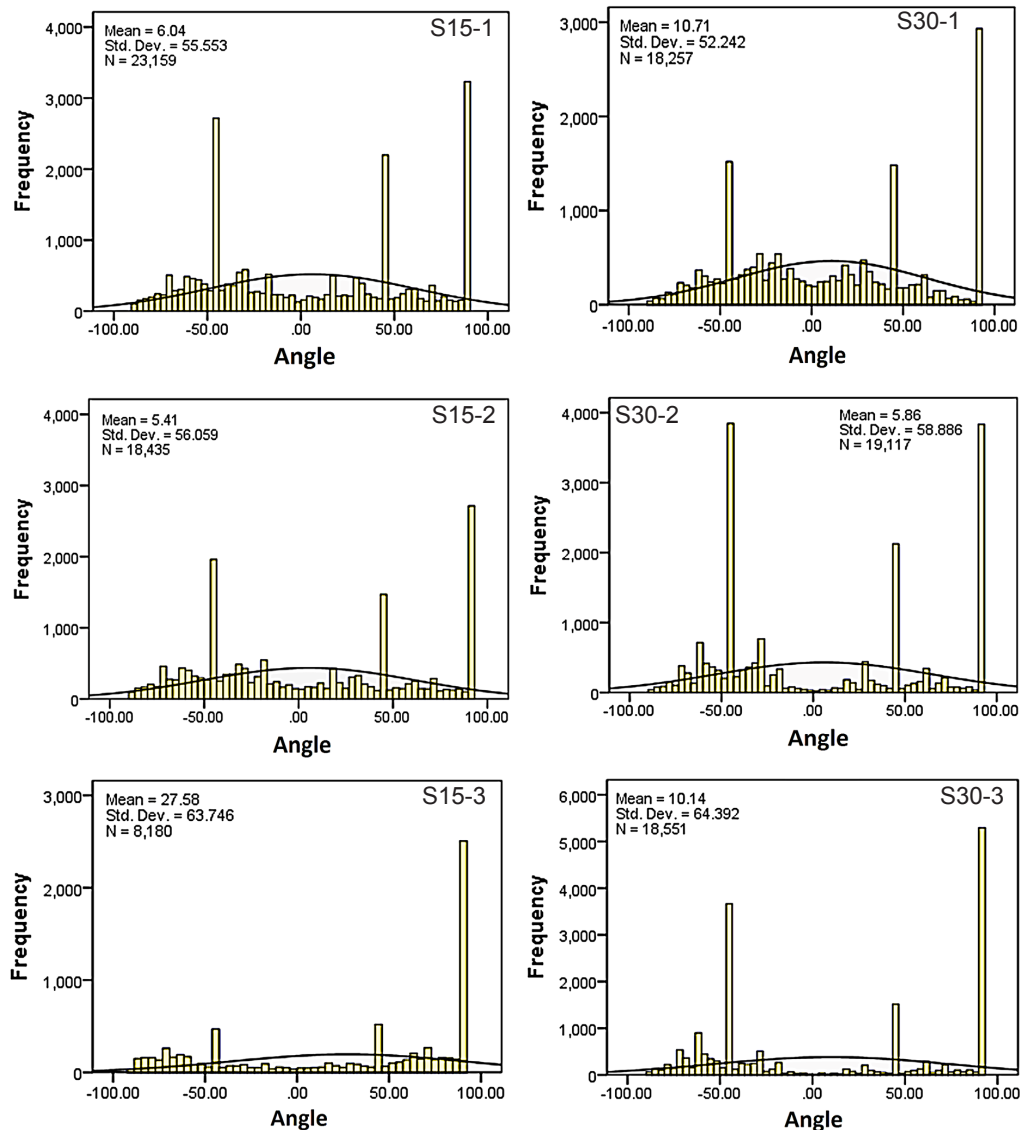

Fig. 6. Fiber orientation distribution.

white objects on a black background (Fig. 5). The measured values of the bonding average area, the bonding dispersion index, and their percentages by the image processing method are presented in Table IV.

A weight gains of 15 g to 30 g in the two samples S30-1 and S15-1 increased the quantity of fibers per area unit and the web density. It can be claimed that, by increasing the web covering, the bonding calendar affected more fibers, and, therefore, every bonded point was closer to the bonding pattern. The values for the bonding average area, presented in Table IV, are suggestive of this matter. However, in a group with the same weighted average and the different degrees of uniformity, a decrease in the surface uniformity led to a reduction in the bonding average area. In other words, with a decrease in the surface uniformity, the possibility of existing empty pores in some areas of the web

is increased. So, when a non-woven web is placed under a thermal bonding calendar, some of the calendar bumps occur in the empty pores. This prevents the formation of bonding points, and, even if they are formed, they will be sketchy. It also reduces the bonding average area and the bonding percentage, which, in consequence, affects the relevant statistical indicators. All this leads to the reduced possibility of forming uniform bonding points, which in this regard is confirmed by the presented dispersion index. To sum up, the lower bonding uniformity, the lower surface uniformity, thus, the higher bonding dispersion index.

D. Fiber Orientation Results
The results for RF method are presented in Fig. 6. It appears that, in each group with the same weighted average, the distribution of fibers orientation is better in samples with
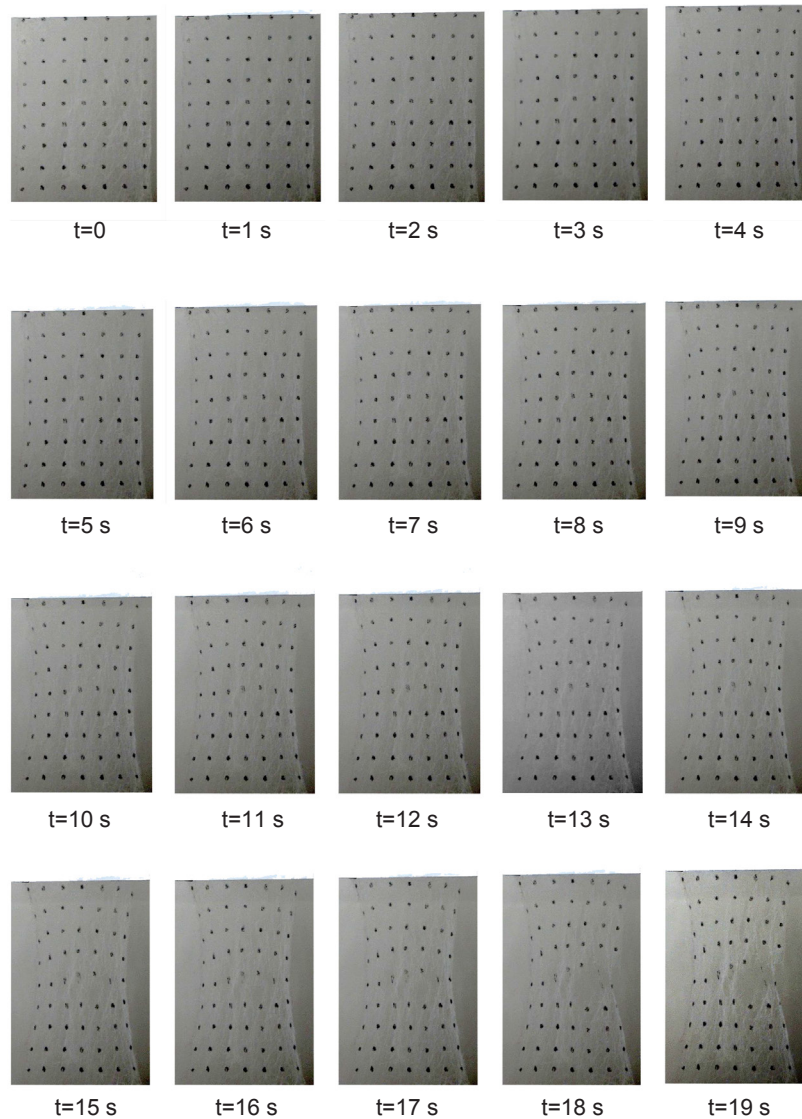

Fig. 7.   Sequence images of S15-3 sample during tensile testing.

more uniformity.

The fibers are also distributed at various angles rather than being highly oriented in a specific direction. This is consistent with the results gained through actual observation. However, for a sample with more non-uniformity, the fibers are not distributed at various angles and are oriented in a certain direction. As it is clearly shown in the charts, the frequency is the highest at some angles. The original pictures suggest that the results derived from RF to characterize the orientation match the findings coming through practical observation.

E. Local Displacement Results During Tensile Testing

The sequence images of sample S15-3 during tensile testing are presented in Fig. 7, and the 3D charts of local displacement for the marked dots are shown in Fig. 8. Many structural parameters affect the fabric tensile properties. During the tensile testing of non-woven samples, the breaks began at critical points, such as weak link points, non-uniform surface and etc. The probability of critical points in a non-uniform sample is very high. Therefore, the tensile strength will be less, and the breaks happen at the critical point. In the final images of Fig. 9, it is clear that a break leads to the local displacement of some marked dots, and that occurs in 17 s to 19 s. These displacements appear as peaks within the same number of seconds as in the 3D chart (Fig. 8). These results hold true for all sample cases. In the present study, it was observed that, in each group with the same weighted average, for a sample with further surface uniformity, the local displacements of the marked dots were equal. Also, there were no critical points for breaks and no peak in the 3D charts. Conversely, in a sample with the lowest surface uniformity, there were more critical points for tension concentration. So, the breaks happened faster, and the displacement charts had several peaks.

F. Tensile Testing Results

A tensile test and the stress and strain at peak were conducted to investigate the effects of surface uniformity, bonding uniformity, and fiber orientation on the tensile properties of the samples. The mean stress-strain curves as well as the stress and strain at peak for 10 specimens of each sample are presented in Fig. 9.
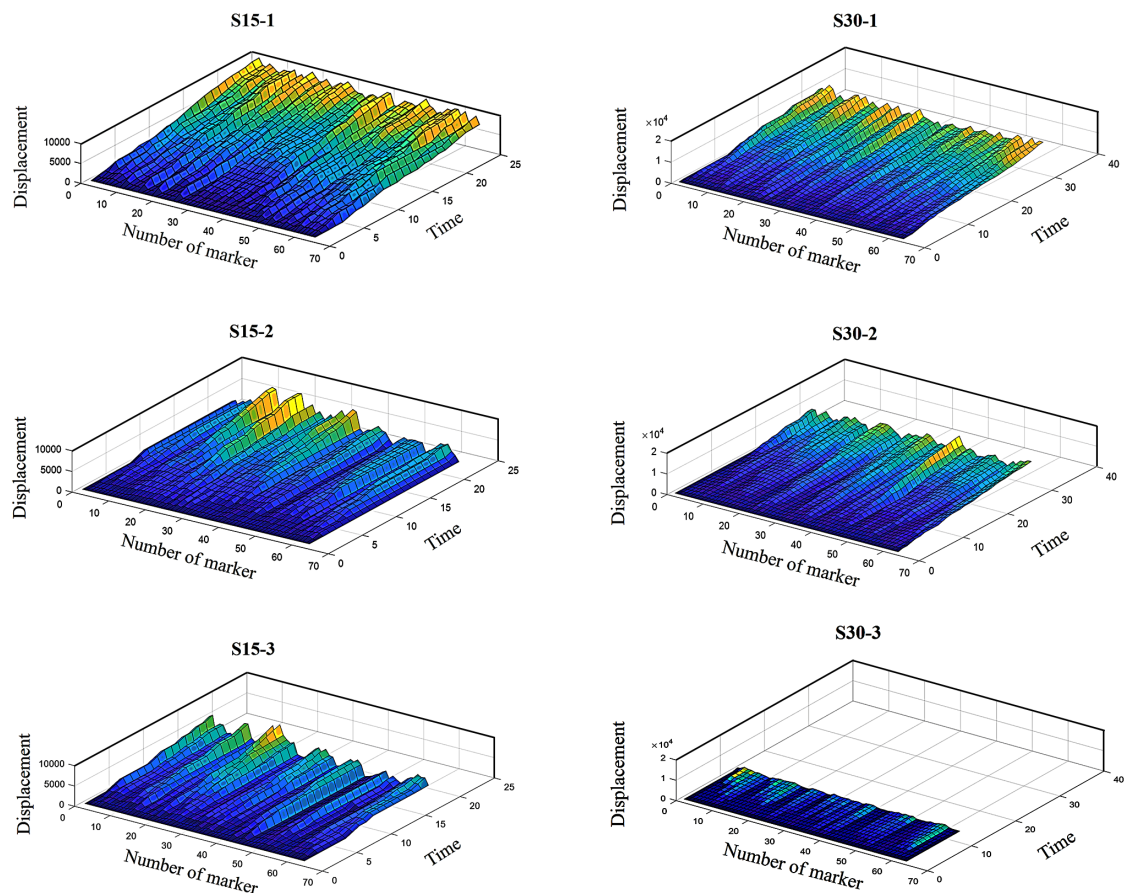

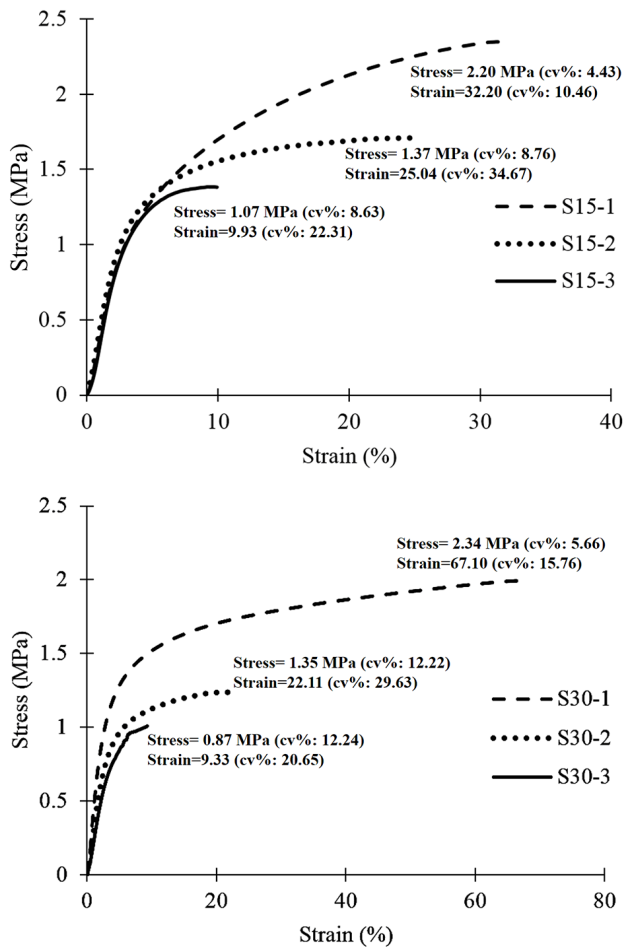Fig. 8. 3D Chart for local displacement during tensile testing.

Fig. 9. Mean stress-strain curves.

elongation-at-break. The important issue is the downtrend of stress and strain in each weighting group, which is consistent well with the degree of samples uniformity.

In general, it can be concluded that the surface dispersion index and the bonding dispersion index are increased in each weighting group, but the percentage of bonding and the stress and strain-at-peak are decreased in pace with a decrease in the degree of the surface uniformity dispersion index and the orientation distribution. A sample which presents poor results during tensile testing and proves to have the worst structural and bonding properties in the image processing method has the worst tensile properties. This suggests that tensile properties are lower in the case of less surface uniformity, fewer bonding structures, worse orientation and more critical points.

IV. CONCLUSION

Due to the lack of an affordable online method for measuring the uniformity of non-woven fabrics, this paper has aimed at, whether a digital imaging processing system can be used to measure non-woven structural characteristics and to estimate tensile properties. We have investigated surface uniformity by the quadrant method (i.e. a method devised for evaluation of surface uniformity). The results indicate that a scanner can be used to measure the surface uniformity for non-woven polypropylene fabrics at web weights ranging from 15 g/m^2 to 30 g/m^2. In the image processing of the bonding points uniformity, it was observed that a sample with a higher surface uniformity has a lower bonding dispersion index, a higher bonding average area, and a higher bonded zones percentage. The distribution of fiber orientation was evaluated using regionprops function method, and it was indicated that the samples with more uniformity have a better fiber orientation distribution. In the digital image correlation of sequence images during tensile testing, it was observed that, in each group with the same weighted average, for a sample with further surface uniformity, the marked dots were equal in terms of their local displacement. Also, there were no critical points for breaks and no peak in the 3D charts. Conversely, in the sample with the lowest surface uniformity, there were more critical points for tension concentration, the breaks happened faster, and the displacement charts had several peaks. The stress and strain at peak were decreased by a decrease in the degree of uniformity. In stress and strain measurements, it was found that, for a sample with more weight, the CV% value is lower, and a sample with a medium surface uniformity has a higher CV% value than a sample with the highest surface uniformity. However, a sample with the lowest uniformity has a lower CV% value than a sample with a medium uniformity. Less uniformity

According to Fig. 9, in each group of samples with the same weighted average, a sample with the further uniformity shows higher stress and strain. By comparing the presented coefficients of variation (CV%) for stress and strain at peak, it emerges that, for a sample with more weight, the CV% value is lower. It can be claimed that, with an increase in the weight, the possibility of the surface uniformity and the uniformity of thermally-bonded points is increased, and, consequently, the dispersion of tensile properties is reduced. On the other hand, in each group of samples with the same weighted average, it seems obvious for a sample with a medium surface uniformity to have a higher CV% value than a sample with the highest surface uniformity. However, a sample with the lowest surface uniformity has a lower CV% value than a sample with a medium uniformity. It may be because these samples have an extreme non-uniformity in their structures and are broken fast in a certain period of time, which makes the CV% values of these samples lower than those of the samples with a medium uniformity. Samples with a poor surface uniformity have a brittle mode and a very low

or a worse bonding structure would mean more critical points for tension concentration, a bad fiber orientation and, therefore, lower tensile properties. This is a significant point that needs to be considered when adjusting a technique for an on-line application. By changing the product, the lack of uniformity, if any, is recognized, and corrections are made on the production line quickly. This is how large production of shoddy products can be prevented. Applying the image processing method to online quality control is a very useful and effective method that can help the owners of factories to save time and money on quality control.

REFERENCES

[1]   G. Sun, X. Sun, and X. Wang, "Study on uniformity of a melt-blown fibrous web based on an image analysis technique", *e-Polymers*, vol. 17, no. 3, pp. 211-214, 2017.

[2]   K. Yildiz, A. Buldu, M. Demetgul, and Z. Yildiz, "A novel thermal-based fabric defect detection technique", *J. Text. Inst.*, vol. 106, no. 3, pp. 275-283, 2015.

[3]   S. Li, H. Yi, and S. Shang, "Measurement of diameter and scale of cashmere fibers by computer image analysis", *J. Fiber Bioeng. Inform.*, vol. 5, no. 1, pp. 95-103, 2012.

[4]   H. Merbold, D. Maas, and J. Van Mechelen, "Multiparameter sensing of paper sheets using terahertz time-domain spectroscopy: caliper, fiber orientation, moisture, and the role of spatial inhomogeneity", In: *IEEE Sensors 2016,* Orlando, FL, USA, pp. 1-3, 2016.

[5]   R. Veerabadran, H. Davis, S. Batra, and A. Bullerwell, "Devices for on-line assessment of nonwovens' basis weights and structures", *Text. Res. J.*, vol. 66, no. 4, pp. 257-264, 1996.

[6]   P.A. Boeckerman, "Meeting the special requirements for on-line basis weight measurement of lightweight nonwoven fabrics", *Tappi J.*, vol. 75, no. 12, pp. 166-172, 1992.

[7]   H.-C. Lien and C.-H. Liu, "A method of inspecting non-woven basis weight using the exponential law of absorption and image processing", *Text. Res. J.*, vol. 76, no. 7, pp. 547-558, 2006.

[8]   J. Liu, B. Zuo, X. Zeng, P. Vroman, and B. Rabenasolo, "Nonwoven uniformity identification using wavelet texture analysis and LVQ neural network", *Expert Syst. Appl.*, vol. 37, no. 3, pp. 2241-2246, 2010.

[9]   J. Liu, B. Zuo, X. Zeng, P. Vroman, and B. Rabenasolo, "Wavelet energy signatures and robust bayesian neural network for visual quality recognition of nonwovens", *Expert Syst. Appl.*, vol. 38, no. 7, pp. 8497-8508, 2011.

[10]   J. Liu, B. Zuo, X. Zeng, P. Vroman, and B. Rabenasolo, "Visual quality recognition of nonwovens using generalized gaussian density model and robust bayesian neural network", *Neurocomputing*, vol. 74, no. 17, pp. 2813-2823, 2011.

[11]   B. Pourdeyhimi and L. Kohel, "Area-based strategy for determining web uniformity", *Text. Res. J.*, vol. 72, no. 12, pp. 1065-1072, 2002.

[12]   E. Amirnasr, E. Shim, B.-Y. Yeom, and B. Pourdeyhimi, "Basis weight uniformity analysis in nonwovens", *J. Text. Inst.*, vol. 105, no. 4, pp. 444-453, 2014.

[13]   S. Nohut and T. Arici, "Estimation of areal weight, grab tensile strength, and elongation at break of PP spunbond nonwovens using digital image analysis and artificial neural networks", *J. Eng. Fabr. Fibers (JEFF)*, vol. 10, no. 2, 2015.

[14]   M. Taşcan and S. Nohut, "Nondestructive prediction of areal weight, grab tensile strength and elongation at break of polypropylene (pp) spunbond nonwoven fabrics using digital image analysis", *J. Text. Appar./ Tekstil ve Konfeksiyon*, vol. 25, no. 1, 2015.

[15]   N. Mao and S. Russell, "Directional permeability in homogeneous nonwoven structures part I: the relationship between directional permeability and fibre orientation", *J. Text. Inst.*, vol. 91, no. 2, pp. 235-243, 2000.

[16]   R. Murugan and S. Ramakrishna, "Design strategies of tissue engineering scaffolds with controlled fiber orientation", *Tissue Eng.*, vol. 13, no. 8, pp. 1845-1866, 2007.

[17]   B. Pourdeyhimi, R. Ramanathan, and R. Dent, "Measuring fiber orientation in nonwovens: part I: simulation", *Text. Res. J.*, vol. 66, no. 11, pp. 713-722, 1996.

[18]   B. Pourdeyhimi, R. Ramanathan, and R. Dent, "Measuring fibre orientation in nonwovens, part II: direct tracking", *Text. Res. J.*, vol. 67, no. 3, pp. 181-190, 1996.

[19]   B. Pourdeyhimi, R. Dent, and H. Davis, "Measuring fiber orientation in nonwovens part III: fourier transform", *Text. Res. J.*, vol. 67, no. 2, pp. 143-151, 1997.

[20]   B. Pourdeyhimi and R. Dent, "Measuring fiber orientation in nonwovens part IV: flow field analysis", *Text. Res. J.*, vol. 67, no. 3, pp. 181-187, 1997.

[21]   B. Pourdehyhimi, R. Dent, A. Jerbi, S. Tanaka, and A. Deshpande, "Measuring fiber orientation in nonwovens part V: real webs", *Text. Res. J.*, vol. 69, no. 3, pp. 185-192, 1999.

[22]   A.A. Jeddi, H. Kim, and B. Pourdeyhimi,

"Measurement of fiber orientation in nonwovens optical fourier transform", *Int. Nonwovens J.*, vol. 10, pp. 10-16, 2001.

[23] M. Tunák, J. Antoch, J. Kula, and J. Chvojka, "Estimation of fiber system orientation for nonwoven and nanofibrous layers: local approach based on image analysis", *Text. Res. J.*, vol. 84, no. 9, pp. 989-1006, 2014.

[24] O. Stolyarov and S. Ershov, "Characterization of change in polypropylene spunbond nonwoven fabric fiber orientation during deformation based on image analysis and fourier transforms", *J. Strain Anal. Eng. Des.*, vol. 52, no. 8, pp. 457-466, 2017.

[25] W. Peters and W. Ranson, "Digital imaging techniques in experimental stress analysis", *Opt. Eng.*, vol. 21, no. 3, pp. 213427, 1982.

[26] Z. Zhou, P. Chen, F. Huang, and S. Liu, "Experimental study on the micromechanical behavior of a PBX simulant using SEM and digital image correlation method", *Opt. Lasers Eng.*, vol. 49, no. 3, pp. 366-370, 2011.

[27] H. Koerber, J. Xavier, and P. Camanho, "High strain rate characterisation of unidirectional carbon-epoxy IM7-8552 in transverse compression and in-plane shear using digital image correlation", *Mech. Mate*r., vol. 42, no. 11, pp. 1004-1019, 2010.

[28] F. Pierron, M. Sutton, and V. Tiwari, "Ultra high speed DIC and virtual fields method analysis of a three point bending impact test on an aluminium bar", *Exp. Mech.*, vol. 51, no. 4, pp. 537-563, 2011.

[29] J. MacQueen, "Some methods for classification and analysis of multivariate observations", In *Proceedings of the Fifth Berkeley Symposium on Mathematical Statistics and Probability*, vol. 1, Statistics, Berkeley, California, USA, pp. 281-297, 1967.

[30] D.L. Davies and D.W. Bouldin, "A cluster separation measure", *IEEE Transact. Pattern Anal. Mach. Intell.*, no. 2, pp. 224-227, 1979.

[31] A. Hore and D. Ziou, "Image quality metrics: PSNR vs. SSIM", In: *20th International Conference on Pattern Recognition (ICPR 2010)*, pp. 2366-2369, 2010.

[32] M.A. Sutton, J.J. Orteu, and H. Schreier, *Image Correlation for Shape, Motion and Deformation Measurements: Basic Concepts, Theory and Applications*, Springer Science & Business Media, 2009.